

Synthesis and Study of a New Type of Fluorinated Polyether Demulsifier for Heavy Oil Emulsion Demulsification

Lixin Wei, Lin Zhang,* Shijun Guo, Xinlei Jia, Yu Zhang, Chao Sun, and Xuanrui Dai



Cite This: *ACS Omega* 2021, 6, 25518–25528



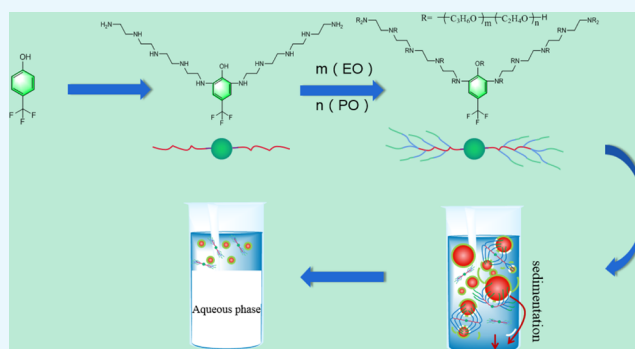
Read Online

ACCESS |

Metrics & More

Article Recommendations

ABSTRACT: To solve the problem of heavy oil demulsification difficulties in Liaohe Oilfield, phenolamine resin initiator was synthesized from *p*-trifluoromethyl phenol, and then FB series fluorinated polyether demulsifiers were synthesized by block polymerization using ethylene oxide (EO) and propylene oxide (PO) as raw materials. The demulsifiers were characterized by infrared spectroscopy, cloud point, hydrophilic–lipophilic balance (HLB) value, and surface tension. The demulsifying and dehydrating properties were tested by demulsifying and dehydrating experiments, the demulsification mechanism was analyzed by the microscopic demulsification process test, and the influence of demulsifier addition and demulsifying temperature on demulsifying performance was also studied. The results showed that under the condition of the optimum demulsification temperature of 60 °C and the optimum demulsifier dosage of 100 mg/L, the water removal (%) of fluorinated polyether demulsifier of FB 4 was the highest, and the overall water removal (%) of 50 mL crude oil emulsion in Liaohe Oilfield reached 90.33% within 2 h, which was



better than the current demulsifier used in Liaohe crude oil.

INTRODUCTION

Crude oil is one of the most important strategic energy substances in the world, and its demand is increasing with the rapid development of all countries.^{1–3} In the process of oil exploitation, it is difficult to avoid mixing the produced crude oil with water.⁴ The natural emulsifiers in crude oil, such as colloids, asphaltenes, solid particles, and paraffin crystals, are accompanied by a large amount of formation water.^{5–7} During the exploitation process, relatively stable emulsions are formed due to the effects of temperature, shear, and extrusion.⁸ Eighty percent of the world's crude oil is emulsified from the ground.⁹ These stable emulsions can cause serious corrosion or blockage to plant equipment and pipelines and bring operational and safety problems to oil field production.^{5,10,11} Therefore, it is necessary to demulsify and dehydrate crude oil emulsions during oil field production.

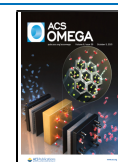
Heavy oil is a kind of unconventional crude oil with large reserves and high exploitation difficulty, which is widely distributed in the United States, Canada, Venezuela, China, and many other countries.^{12–14} On the one hand, heavy oil has high viscosity, high density, high contents of gum and asphaltene, and rigid thick film with better compactness than conventional crude oil emulsion.^{15–17} The interpolymerization behavior of water droplets at the oil–water interface is hindered, which makes the emulsion very stable and difficult to demulsify and dehydrate.¹⁸ On the other hand, the developed heavy oil is fully stirred with water through the strong shear

action of the pipeline to form a complex and stable emulsion.^{19,20} At present, the commonly used methods of demulsification and water removal mainly include physical method, chemical method, and biological method.^{21–23} The chemical demulsification method is widely used in oil field demulsification because of its convenience and efficiency. It is the most common and most studied demulsification technology at present.^{24–26} Sun et al. prepared a novel polyether–polyquaternium (PPA) demulsifier for demulsifying the O/W emulsion that originates from wastewater produced from alkaline–surfactant–polymer (ASP) flooding. When processing an O/W emulsion that contained 500 mg/L oil, this PPA demulsifier exhibited a demulsification efficiency of 80.6% at a 110 mg/L dosage.²⁷ Wu et al. prepared a novel PPS@ZIF-8 demulsifier by grafting branched polyether polysiloxane (PPS) molecules onto the ZIF-8 crystal. When processing simulated water produced from alkaline–surfactant–polymer (ASP) flooding that contained 0.4 g/L oil, the demulsifier exhibited an oil removal rate of 90.03%.²⁸ Li et al.

Received: July 5, 2021

Accepted: September 10, 2021

Published: September 23, 2021



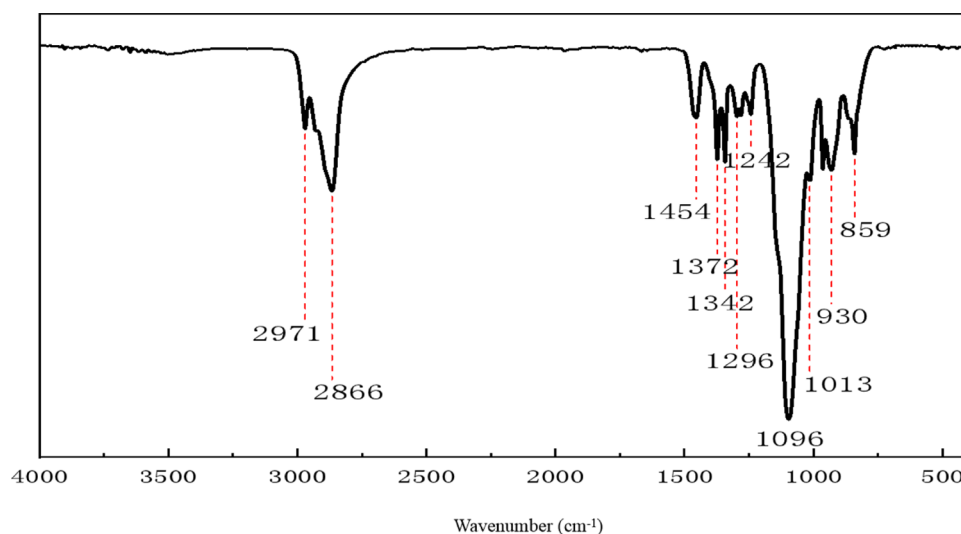


Figure 1. FTIR spectra of FB 1 demulsifier.

synthesized a novel polyether demulsifier with rich oxygen by simple esterification and polymerization. The polyether demulsifier performs well in enhancing the demulsification of the IAA-stabilized (interfacially active asphaltenes) emulsion, achieving complete water removal of the emulsions in 30 min at 60 °C and 400 ppm.²⁹ Polyether demulsifiers can be divided into amines, alcohols, alkyl phenol resins, phenolamine resins, and hydrogen-containing silicone oils according to different initiators.^{30,31} Poly(propylene oxide)–poly(ethylene oxide) and poly(propylene oxide)–poly(ethylene oxide)–poly(propylene oxide) (PPO–PEO and PPO–PEO–PPO, respectively) block polyethers have good compatibility, mainly through the polymerization reaction of the starting agent and propylene oxide and ethylene oxide, which played an important role in crude oil demulsification, emulsification cleaning, sewage treatment, and other areas.^{32,33} The properties of block polyether surfactants are closely related to the structure of the initiator.³⁴ Linear, multibranch, dendriform polymers can be synthesized according to the amount and location of active hydrogen in the initiator.^{35,36}

Fluorinated polyether demulsifier is one of the most important special surfactants and has the highest activity.³⁷ Perfluoroalkyl and polyfluoroalkyl substances (PFASs) are a new class of persistent organic pollutants, which pose great harm to the environment and biological health.³⁸ However, fluorinated substances have high surface activities and are indispensable social resources in social production and life. High use of fluorinated substances is of great significance to industrial production.^{39,40} In the process of oil field production, the addition of fluorine-containing demulsifier is very small, and through sewage treatment, such as adsorption method and conversion method, the fluorine content in sewage can reach the emission standard, thereby reducing the harm to the ecological environment.^{41,42} Fluorinated surfactants have the characteristics of high surface activity, strong thermal stability and chemical inertia, and hydrophobicity and oilphobicity, so fluorinated demulsifiers have high demulsifying and water removal capacities.^{43–45} Song et al. synthesized new multibranch–linear–multibranch fluorinated copolymer demulsifiers and found that the amphiphobic effect of the fluoride group not only accelerated the diffusion process of polymer molecules from the bulk to the interface but also

reduced the rigidity of the interface film by repelling the original interface active material and producing effective fracturing.⁴⁶ Xu et al. synthesized a series of functional fluorinated graphene (FG) materials including urea-modified FG (UFG), alkali-modified FG (AFG), and hydrazine hydrate-modified FG (HFG) with different fluorine contents. The results showed that the demulsification efficiency increased with a decrease in the fluorine content of functional FG and that the oil concentration in the separated water phase decreased to the lowest value when 600 mg/L HFG was added into the wastewater.⁴⁷ Zhang et al. synthesized novel branched fluorinated cationic, amphoteric, gemini, amine oxide, and anionic surfactants using perfluoro-2-methyl-2-pentene as a starting material. The results showed that each surfactant boasted good surface activity (they had a reduced surface tension of water as low as 19.88 mN/m) and salt resistance. Fluorinated surfactants are more efficient than traditional surfactants since they show high surface performances at a low critical micelle concentration (CMC).⁴⁸

The new fluorinated polyether demulsifier prepared in this study has high surface activity, which can preferentially adsorb and destroy the original oil–water interface film, reduce the stability of the emulsion, increase the interaction of adjacent water droplets, coalesce into large water droplets to settle, and complete the oil–water separation. In this study, a series of fluorinated polyether demulsifiers were synthesized by the polymerization reaction of p-trifluoromethyl phenol and EO and PO. The demulsifying and water removal capacity of the demulsifiers was tested, and the factors affecting the demulsifying performance were studied. The demulsifiers have a simple preparation process and good demulsification effect, which are superior to the conventional demulsifier without fluorine in Liaohe Oilfield.

RESULTS AND DISCUSSION

Fourier Transform Infrared (FTIR) Spectra of Demulsifier. Since the FTIR spectra shapes of polyether demulsifiers with different EO and PO contents in the same series are basically the same, only the absorption peak intensity of characteristic groups is slightly different, so only the infrared spectrum diagram of FB1 is given, as shown in Figure 1.

By observing the FTIR spectra of FB 1, it can be seen that the $-\text{CH}$ stretching vibration absorption peak is at 2971 cm^{-1} , the stretching vibration absorption peak and bending vibration peak of $-\text{CH}_2$ are at 2866 and 1454 cm^{-1} , respectively, and the symmetric deformation absorption peak of $-\text{CH}_3$ is at 1372 cm^{-1} . The peak at 1342 cm^{-1} is attributed to the $\text{C}-\text{N}$ bond stretching vibration, the peak at 1296 cm^{-1} is due to the $-\text{CH}_2$ out-of-plane bending vibration, the peak at 1242 cm^{-1} corresponds to the characteristic peak of aromatic ether, and the peaks at 1096 and 930 cm^{-1} are $\text{C}-\text{O}-\text{C}$ asymmetrical and symmetric stretching vibration absorption peaks. The peak at 859 cm^{-1} corresponds to the plane oscillations of $-\text{CH}_2\text{O}-$, and the absorption peak at 1013 cm^{-1} indicates the existence of side chains on the ether bond. Combined with the absorption peak at 1372 cm^{-1} , the presence of propylene oxide in the structure can be confirmed and the synthesized substance is consistent with the target product.

Hydrophilic–Lipophilic Balance (HLB) Values and Cloud Point. The turbidity of aqueous solutions of FB series polyether demulsifiers at different temperatures was obtained by experiments. Figure 2 shows turbidities and temperatures of six kinds of demulsifiers.

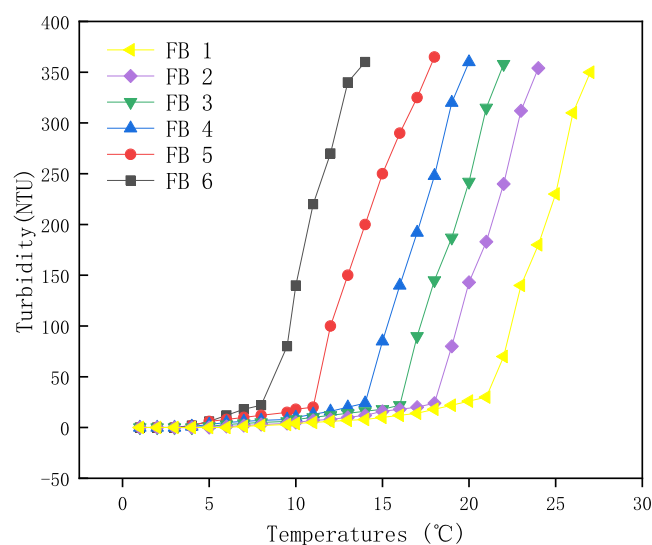


Figure 2. Turbidity of FB series demulsifiers at different temperatures.

It can be seen from Figure 2 that the turbidity of the aqueous solution of FB series polyether demulsifiers increases with an increase in temperature. When the critical temperature is reached, the turbidity increases rapidly and the solution becomes cloudy at the same time. The critical temperature at this time is called the cloud point. The cloud points of FB 1–FB 6 are 21.2, 17.8, 16, 13.9, 10.8, and 8.4 °C, respectively. By comparing the turbidity curves of FB 1, FB 3, FB 5 and FB 2, FB 4, FB 6, it can be found that the cloud point of demulsifier reduces. This is because the PO group is the hydrophobic group, which can reduce the solubility of the aqueous solution, so the cloud point also decreases.⁴⁹ Therefore, when the content of EO is constant, the cloud point decreases with the increase of the content of PO. The EO group is the hydrophilic group, which can promote the hydrogen-bonding force with water so that the cloud point increases. When the PO content is certain, the cloud point decreases with the decrease of the EO content.⁵⁰

The HLB value refers to the characterization of the hydrophilic and lipophilic properties of polyethers.⁵¹ A large HLB value indicates the strong hydrophilic properties of polyethers, while a small value indicates the strong lipophilic properties. The HLB values of the FB series polyether demulsifiers are shown in Table 1.

Table 1. Cloud Point and HLB Values of Series Samples

demulsifiers	initiator:PO	PO:EO	cloud point	HLB
FB 1	1:99	2.7:1	21.2	6.10
FB 2	1:99	3.7:1	17.8	5.76
FB 3	1:159	2.7:1	16	5.59
FB 4	1:159	3.7:1	13.9	5.38
FB 5	1:199	2.7:1	10.8	5.08
FB 6	1:199	3.7:1	8.4	4.84

Surface Tension of FB Series Polyether Demulsifier.

Figure 3 shows that the surface tension of FB series polyether demulsifiers is basically similar. Figure 3A for the FB series different surface tension of polyether demulsifiers in aqueous solution at 25 °C, the surface tension of the polyether demulsifiers decreased with increasing concentration, shows that the synthesis of polyether demulsifiers with high surface activity, can effectively reduce the surface tension of solution. The first inflection point is around 1 mg/L, and the second inflection point is around 100 mg/L. The second inflection point is generally considered to be the CMC (critical micellization concentration) value of the polyether.^{52,53} Before the polyether concentration reached the first inflection point, surface tension drops rapidly with the increase of the concentration of polyether, polyether concentration reached between the two inflection point, surface tension is still a certain velocity decreased, but the decline is reduced, when the concentration of polyether more than a second after the inflection point, further reducing declining rate of surface tension, at this time, with the increase of concentration of polyether surface tension slow decline.

Figure 3B shows the curves of surface tension of FB 1 in NaCl, MgCl₂, and CaCl₂ solutions with polyether concentration. The addition of salt solution can effectively reduce the surface tension of FB 1 polyether solution, and the phenomenon of double inflection point disappears, which is due to the presence of a large number of free ions in the salt solution. The reduction ability of CaCl₂ and MgCl₂ is slightly stronger than that of NaCl.⁵⁴ This is because the hydration of calcium and magnesium ions is lower than that of sodium ions, so the solubility of polyether is lower in the presence of sodium ions. In addition, CaCl₂ and MgCl₂ contain two chloride ions, which, as typical salting-out-type ions, show strong water removal capacity.⁵⁵ There are a fewer free water molecules around the polyether molecules, thus reducing the solubility of the polyether.

Under the action of free ions and demulsifier molecules, it gradually embodies the characteristics of ionic surfactant, which leads to the disappearance of the double inflection point.

Figure 3C shows FB 1 under 25, 45, and 65 °C solution surface tension curve with concentration of polyether. As the temperature increases, the second inflection point gradually disappears, as well as with the decrease of the surface tension of the solution. This is because with the increase in temperature, molecular motion becomes more intense in the solution, the molecular interatomic forces due to the increase

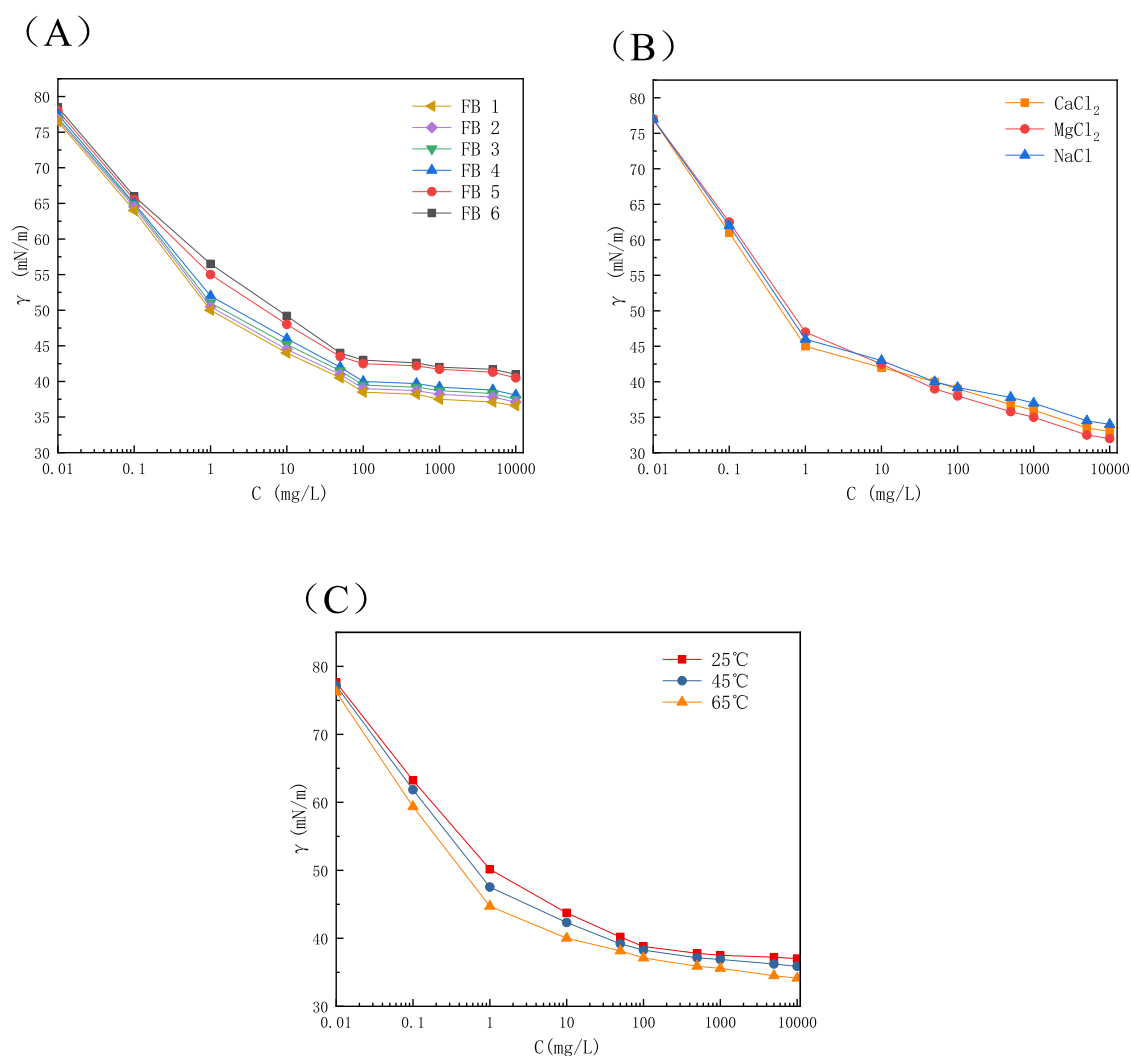


Figure 3. (A) FB series surface tension curve at 25 °C. (B) Surface tension of FB 1 in NaCl, MgCl₂, and CaCl₂ solutions with polyether concentration. (C) Surface tension of FB 1 under different temperature conditions.

of the repulsive force between the molecules reduce, and as a result, the surface tension of the solution decreases.⁵⁶

Demulsification Test. The moisture content of the crude oil emulsion measured by the distillation method is 35.82%. The amount of water removed from the tube during different time periods and the calculated water removal (%) were recorded. The water removal (%) of FB series polyether demulsifier and existing demulsifier in oil field is shown in Figure 4.

As can be seen from Figure 4, the demulsifiers commonly used in the two oil fields have poor effects under the conditions of demulsification temperature of 60 °C and demulsifier dosage of 100 mg/L. AE1910 had the fastest water removal (%) in the first 60 min, but the final water removal (%) was only 69.24%, and LX21 had only 77.32% water removal (%) at 120 min. FB series polyether demulsifiers were all above 40% at 60 min, and the water removal (%) of FB 4 was over 60%. The overall demulsification efficiency of crude oil emulsion in Liaohe Oilfield by FB series polyether demulsifiers reached higher than 85% at 120 min, and the water removal (%) of FB 4 reached 90.33%. The results showed that FB series demulsifiers had a significant effect on the demulsification of crude oil emulsions from Liaohe Oilfield.

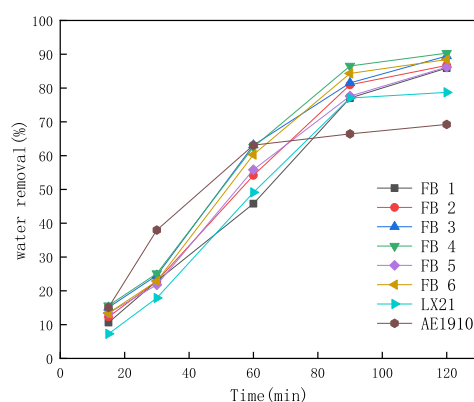


Figure 4. Water removal (%) of FB demulsifier and existing demulsifier at different time periods.

As shown in Figure 5, from the water removal of FB series demulsifiers and two kinds of demulsifiers used in oil fields at different time periods, it can be directly seen that the water removal of FB polyether demulsifiers is the highest in the first 60 min at all time periods, and after 60 min, the amount of water removal decreased gradually. FB 4 polyether demulsifier dehydrates faster than other demulsifiers, and AE1910

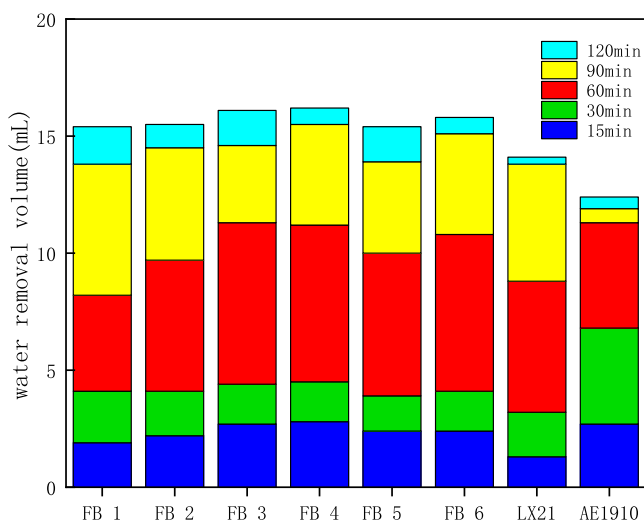


Figure 5. Dehydrated volume of demulsifier per hour.

dehydrates slower than other demulsifiers, although it dehydrates mostly before 60 min.

Microscopic Demulsification Process. The microscopic demulsification process of heavy oil emulsion can be clearly observed in Figure 6. The water removal ability of FB demulsifier is excellent. The heavy oil emulsion was very stable and small water droplets were enveloped in the oil phase. After the addition of FB demulsifier, water droplets of similar size began to aggregate under the action of demulsifier molecules and the size of water droplets also increased significantly. At 30 min, the demulsifier molecule stretched on the oil–water interface, the adjacent water droplets coalesced to form larger water droplets, and the larger water droplets began to absorb the surrounding small water droplets. At 60 min, the droplet size increased further. Finally, after reaching a certain size, large water droplets began to sink under the action of gravity and the demulsification completed.

Demulsification Mechanism. After adding FB series polyether demulsifiers to crude oil emulsions, their molecules pass through the outer phase of the emulsion and diffuse

rapidly to the oil–water interface and adsorb with it. The hydrophilic groups of the demulsifier extend into the water droplet, while the hydrophobic groups remain around the water droplet, as shown in Figure 7. Branches of the demulsifier molecules bridge the droplets so that they can easily get close to each other. With the strong interaction between demulsifier and oil–water interface film, part of the original oil–water interface film was destroyed, removed, and dissociated in the emulsion. The original oil–water interface film consists of asphaltenes, polymers, and other functional reagents that are subsequently added. The demulsifier can make use of hydrophilic groups to aggregate adjacent water droplets. As the protection of these natural emulsifiers is weakened, water droplets in the inner phase begin to aggregate with adjacent water droplets to form larger water droplets. Droplets of similar size tend to cluster together to form larger droplets, and larger droplets can engulf smaller ones around them more quickly. When the droplet size increases to a certain value, they will settle at the bottom of the test tube under the action of gravity to form a water layer. The water layer increases, and the oil and water separate until the water droplets in the emulsion are reduced and the demulsification process ends.

Influence of Demulsification Temperature on Demulsification Performance. Crude oil emulsion (50 mL) and FB 4 demulsifier (100 mg/L) were selected to demulsify at 40, 50, 60, 70, and 80 °C respectively. The demulsifying time was 150 min.

It can be seen from Figure 8 that the water removal effect of demulsifiers increases with an increase in temperature, all less than 20% at 15 min, but increased greatly at 30 min. At 40 °C, the water removal (%) of FB 4 was only 40%, and when the temperature was increased to 60 °C, it increased obviously, over 50% at 30 min, and the highest value was close to 80%. When the temperature was increased again to 70 °C, the demulsification efficiency was also improved, up to 90%. At 70 °C, the water removal (%) and the amount of water removal increased a little, but the increase was not obvious. After 90 min, the water removal (%) was almost the same as that at 60 °C. With the increase in temperature, the diffusion rate of the

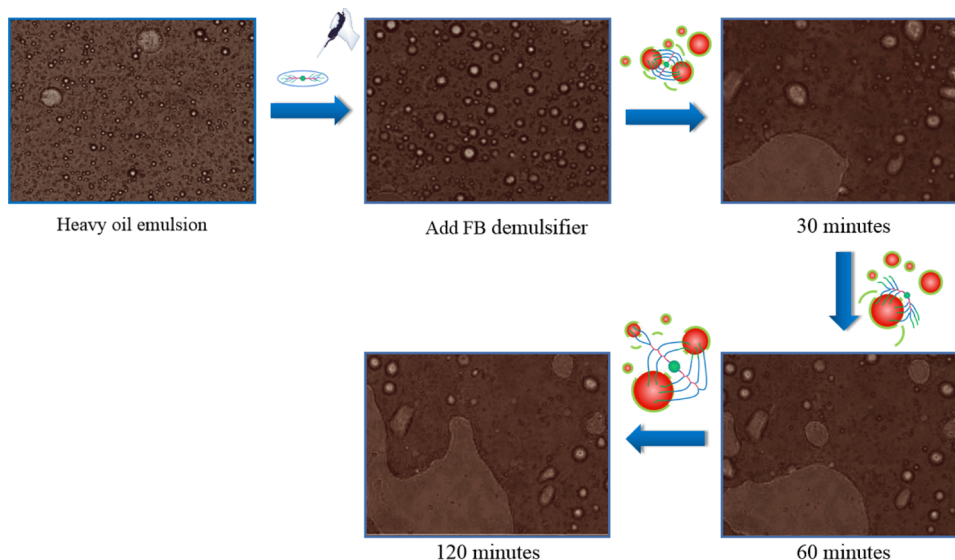


Figure 6. Microscopic demulsification process.

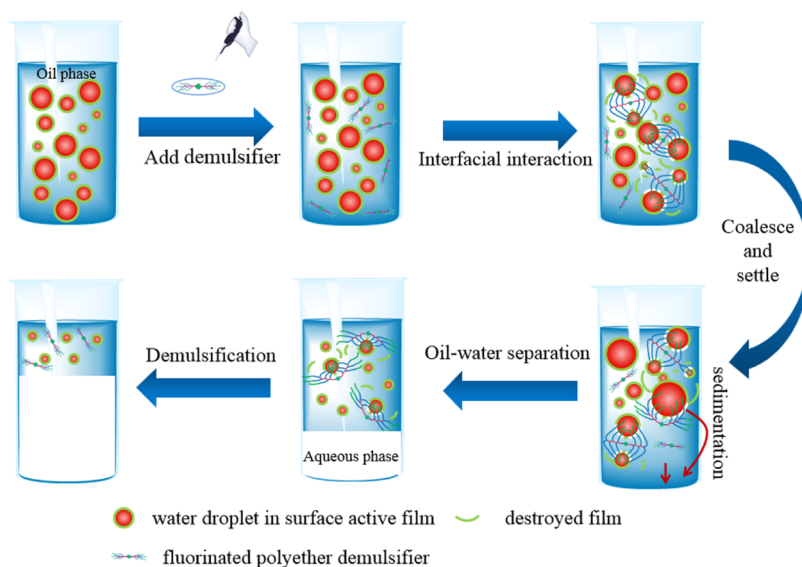


Figure 7. Demulsification mechanism diagram.

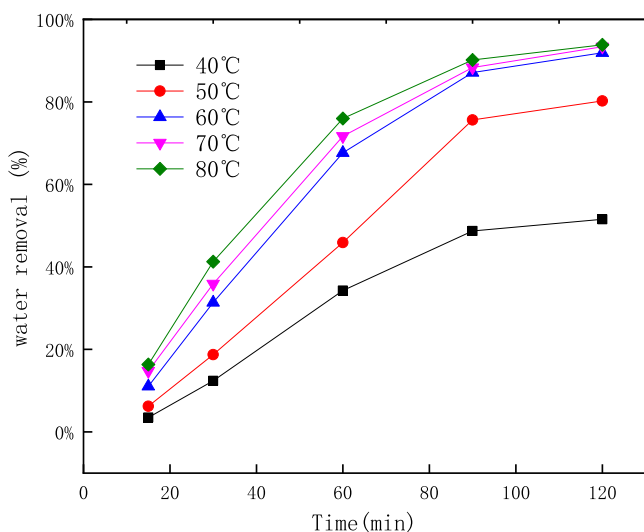


Figure 8. Water removal (%) at different demulsification temperatures of Liaohe crude oil emulsion.

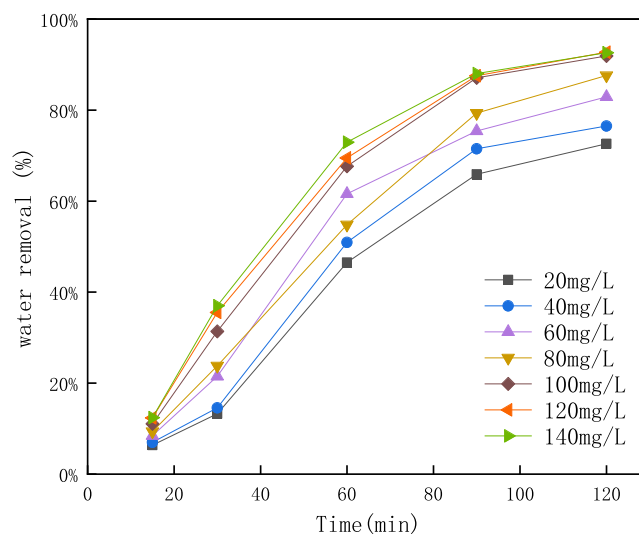


Figure 9. Effect of different demulsifier dosages on demulsification and water removal of Liaohe crude oil emulsion.

demulsifier and the thermal movement of water molecules increase and the viscosity of crude oil emulsion decreases.⁵⁷ At the same time, the increase in temperature also leads to the separation of natural emulsifier molecules from the oil–water interface membrane and the decrease in the interfacial strength; thus, the water droplets become more concentrated. The optimum demulsification temperature was 60 °C, considering that the water removal (%) increased little at 70 °C compared with 60 °C.

Influence of Demulsifier Dosage on Demulsification Performance. The demulsification experiment of Liaohe Oilfield crude oil emulsion was carried out under the condition of demulsification temperature of 60 °C with 50 mL of crude oil emulsion. The influence of the concentration of demulsifying agent on demulsification was discussed by controlling the concentration of FB 4, and the optimum demulsifying concentration was determined.

It can be clearly seen from Figure 9 that the demulsifying effect of FB 4 demulsifier increases with the increase of concentration. When the concentration of demulsifier is lower

than 80 mg/L, the demulsifier has a poor dehydrating effect, and when the concentration of demulsifier is higher than 80 mg/L, the dehydrating effect is obviously improved, up to 90.33%, but when the concentration of demulsifier is higher than 100 mg/L, the dehydrating speed and dehydrating rate are increased and the demulsifier concentration is 140 mg/L, which is lower than 100 mg/L. The reason for this phenomenon is that the number of demulsifier molecules adsorbed on the oil–water interface is related to the concentration of demulsifier.⁵⁸ A high concentration leads to a high molecular weight adsorbed on the oil–water interface membrane, which reduces the stability of the membrane and improves the water removal (%).^{59,60} However, when the adsorption amount at the oil–water interface reaches the saturation value, that is, the critical micelle concentration, micelles are generated inside the oil–water interface membrane; thus, the adsorption amount decreases and the demulsification effect of demulsifier also decreases.⁶¹ There-

Table 2. Basic Physical Properties of Crude Oil Produced in a Block of Liaohe Oilfield

density kg·m ⁻³	dynamic viscosity (50 °C) mPa·s	gum %	asphaltene %	acid value mgKOH·g ⁻¹	pour point °C	moisture content %
943.0	180.2	22.98	12.75	2.45	17	35.82

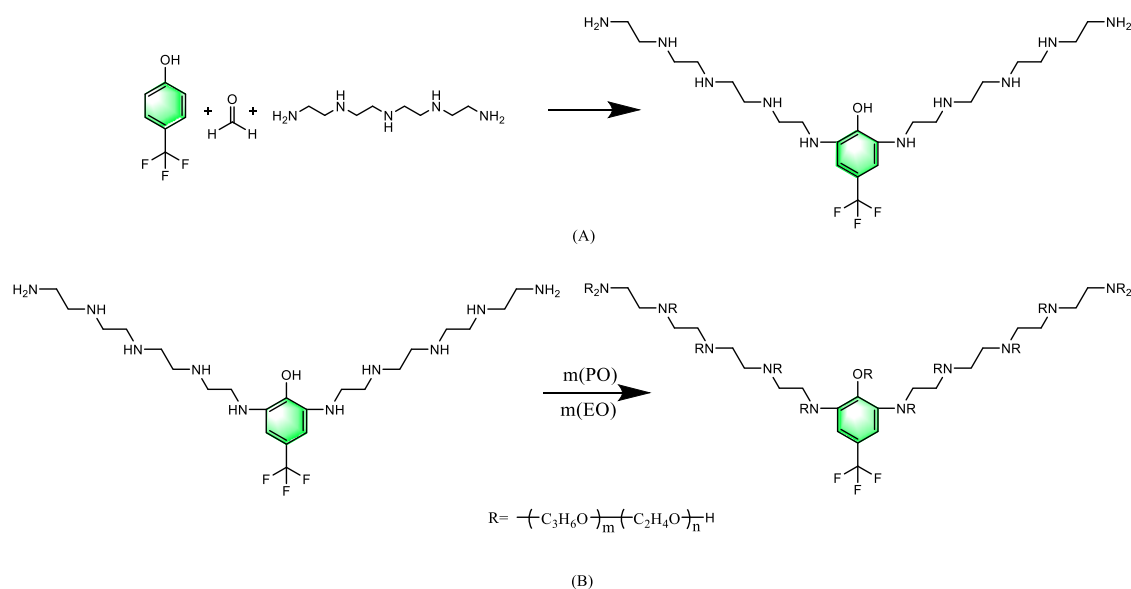


Figure 10. Chemical reaction formula of polyether demulsifier.

fore, for FB 4 polyether demulsifier, the optimal demulsification concentration is 100 mg/L.

CONCLUSIONS

In the face of the increasing complexity of crude oil emulsions, demulsifiers will become increasingly efficient in the future. In this study, FB series fluorinated polyether demulsifiers were synthesized from trifluoromethyl phenol and formaldehyde, and the synthesis of the target demulsifiers was confirmed by FTIR spectra. FB series demulsifiers can effectively reduce the surface tension of the oil–water interface film and destroy the natural polar substances of the oil–water interface, thus achieving the goal of water removal. The water removal experiment of Liaohe Oilfield heavy oil emulsion using FB series polyether demulsifiers was carried out through a bottle test. The optimum demulsification temperature of FB series demulsifiers was obtained by changing the demulsification temperature and increasing the dosage of demulsifier. The optimum dosage of the demulsifier was 100 mg/L, and the water removal (%) of FB 4 was 90.33% at the concentration of 100 mg/L and the temperature of 60 °C, which was superior to the two demulsifiers used in Liaohe Oilfield.

EXPERIMENTAL SECTION

Materials. Tetraethylene pentaamine was purchased from Beijing Tianyu Kanghong Chemical Technology Co., Ltd. *p*-Trifluoromethyl phenol was purchased from Shanghai Sahn Chemical Technology Co., Ltd. Formaldehyde was purchased from Shanghai Macklin Biochemical Technology Co., Ltd. Xylene and toluene were ordered from Shanghai Jizhi Biochemical Technology Co., Ltd. Potassium hydroxide was purchased from Shanghai Sibaiquan Chemical Co., Ltd. Potassium hydroxide was purchased from Shanghai Si Bai Quan Chemical Co., Ltd. Ethylene oxide (EO) and propylene oxide (PO) were purchased from Shandong Zixiang Sales

Chemical Co., Ltd. The tested oil sample was fluid produced from a heavy oil block in Liaohe Oilfield. The physicochemical characteristics are shown in Table 2.

Compared with the raw materials of conventional demulsifier, the *p*-trifluoromethyl phenol material used is more expensive and cannot be applied in large quantities in the whole oil field production process. However, it can achieve efficient demulsification performance for the special heavy oil emulsion in a certain block, which is significantly better than the various demulsifiers used in a certain block of Liaohe Oilfield so as to solve the problem of demulsification and dehydration. *p*-Trifluoromethyl phenol is not a dangerous or control product, and hence easily available. It can meet the needs of medium- and small-scale production.

Synthesis of Fluorinated Polyether Demulsifier. To begin with, 37.8 g of *p*-trifluoromethyl phenol and 74.5 g of tetraethylene pentaamine were put into a three-neck flask, which was placed in an oil bath and heated to 45 °C. After 15 min of heat preservation, 27.6 g of formaldehyde (40 wt %) solution was slowly added into a burette, and the molar ratio of formaldehyde to *p*-trifluoromethyl phenol was 2:1. The solution was kept for 40 min after dropping. Then, 70 g of xylene, which is half the mass of the total material, was added, heated to 110 °C for 2 h, then refluxed to 160 °C for 2 h, and kept for 1 h. After the reaction is complete, a yellowish viscous liquid, namely, fluorine-containing initiator, was obtained. The reaction steps are shown in Figure 10A.

The initiator (5 g) obtained from the above reaction and potassium hydroxide (0.70 g) were added to the reactor at a high temperature and a high pressure. N₂ was employed to replace the air in the reactor. The gas in the high-pressure reactor was pumped out by a vacuum pump, and the pressure indicator was observed to stop when it reached a negative pressure. Epoxy-propane (PO) (495 g) was slowly fed into the feed port and heated to 130 °C, and the pressure gauge reading was maintained at about −0.09 MPa. The feed valve was

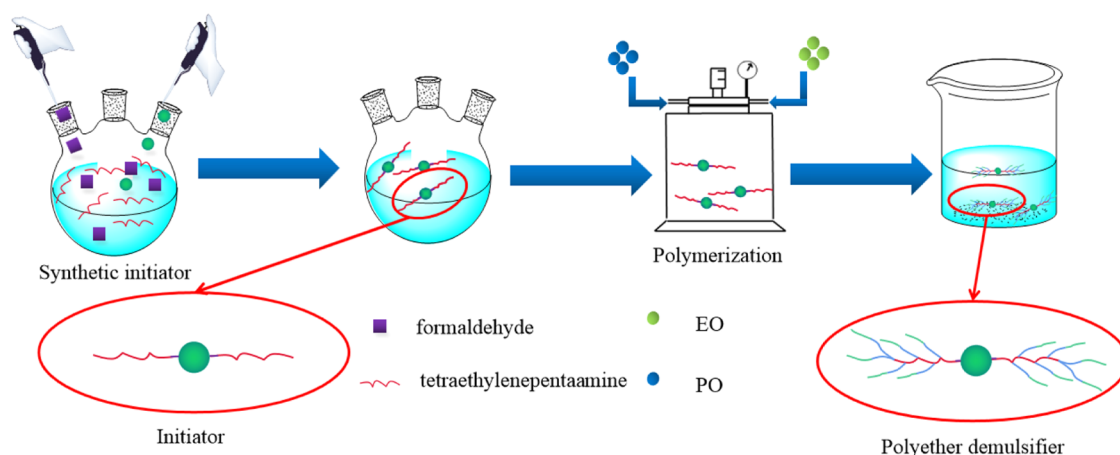


Figure 11. Schematic diagram of the chemical synthesis of polyether demulsifiers.

closed when the feed was completely finished. And the first step of the reaction ended when the pressure indicator was reduced to negative pressure.

Following the first step of the experiment, 0.7 g of potassium hydroxide was put in the high-pressure reactor again and 183.3 g of ethylene oxide (EO) was passed into the reactor in the same way for polymerization reaction. Finally, fluorinated polyether demulsifier FB 1 was obtained by cooling and opening the reactor. The mass ratio of its initiator to propylene oxide (PO) is 1:99, and the mass ratio of propylene oxide (PO) to ethylene oxide (EO) is 2.7:1. The reaction steps are shown in Figure 10B. The schematic diagram of the chemical synthesis of polyether demulsifiers are shown in Figure 11.

In each experiment, the mass ratios of initiator to propylene oxide (PO) were 1:99, 1:159, and 1:199. The mass ratios of propylene oxide (PO) and ethylene oxide (EO) were 2.7:1 and 3.7:1. The quality ratios of initiator to PO and PO to EO of polyether demulsifiers are shown in Table 3.

Table 3. Quality Ratios of Initiator to PO and PO to EO of Polyether Demulsifiers

demulsifiers	initiator:PO	PO:EO	demulsifiers	initiator:PO	PO:EO
FB 1	1:99	2.7:1	FB 4	1:159	3.7:1
FB 2	1:99	3.7:1	FB 5	1:199	2.7:1
FB 3	1:159	2.7:1	FB 6	1:199	3.7:1

Fourier Transformed Infrared (FTIR) Spectra of FB Series Polyether Demulsifiers. The demulsifiers were characterized by a TENSOR27 Fourier transform infrared spectrometer made by Bruker, Germany, and the absorption peaks of different groups were observed.

Determination of Cloud Point and Hydrophilic–Lipophilic Balance (HLB) Value of Demulsifier. *Cloud Point.* The turbidity of 1 wt % aqueous solution of FB series polyether demulsifiers was measured by an HACH2100Q portable turbidity point instrument at different temperatures. A GDH-0506W high-precision low-temperature thermostatic tank was used to heat up the measuring bottle containing polyether aqueous solution. The water bath temperature increased at a span of 0.5 °C from 2 to 10 °C, and when the temperature was higher than 10 °C, it increased at a span of 1 °C. Before each measurement, the water bath was kept at a constant temperature for 10 min, and then it was quickly removed, dried, and put into a turbidity point meter smoothly.

The turbidity at this temperature was measured and recorded. During the test, all of the measured values were plotted. The temperature of turbidity mutation was the cloud point of 1 wt % water solution of the nonionic polyether demulsifier.

The hydrophilic–lipophilic balance (HLB) value of polyether demulsifiers has a certain quantitative relationship with the cloud point. The HLB value can be calculated from the cloud points obtained in the above experiments, and the calculation formula is given in eq 1.⁶²

$$\text{HLB} = 0.0980X + 4.02 \quad (1)$$

where X is the cloud point value of 1 wt % polyether demulsifier FB.

Determination of Interfacial Tension of Demulsifier. The Kruss DSA100 contact angle-measuring instrument was used for measuring polyether demulsifiers. The polyether aqueous solutions with different concentrations were heated in a water bath after being prepared and then measured at a set temperature of 25 °C. A 1 mL disposable syringe was selected as the instrument of the hanging drop method to measure the interfacial tension of polyether aqueous solutions with different concentrations.

Experiment on Demulsification and Water Removal of Demulsifier. Determination of water content in crude oil emulsion: The emulsion was heated to flow at 35 °C and poured into a round-bottom flask containing diesel oil with a few shards of porcelain at the bottom to prevent the liquid from boiling over. A condensing tube and receiver were installed, the distillation flask was heated in a constant-temperature oil bath, and the drop rate of the condensate was controlled to approximately four drops per second until there was no more water in the distillation unit and the volume of the liquid in the receiver had not changed for a period of time. Heating was stopped and the mixture was cooled to room temperature. The water droplets attached to the receiver were scraped into the liquid with a tool, and the volume of water in the receiver was read. The volume fraction of water in the crude oil emulsion was calculated according to formula 2.⁶³

$$\varphi = \frac{(V_1 - V_0)}{V} \times 100\% \quad (2)$$

where φ is the volume fraction of water, V_1 is the volume of separated water of blank experimental control, V_0 is the volume of separated water in the receiver, and V is the volume of the crude oil emulsion.

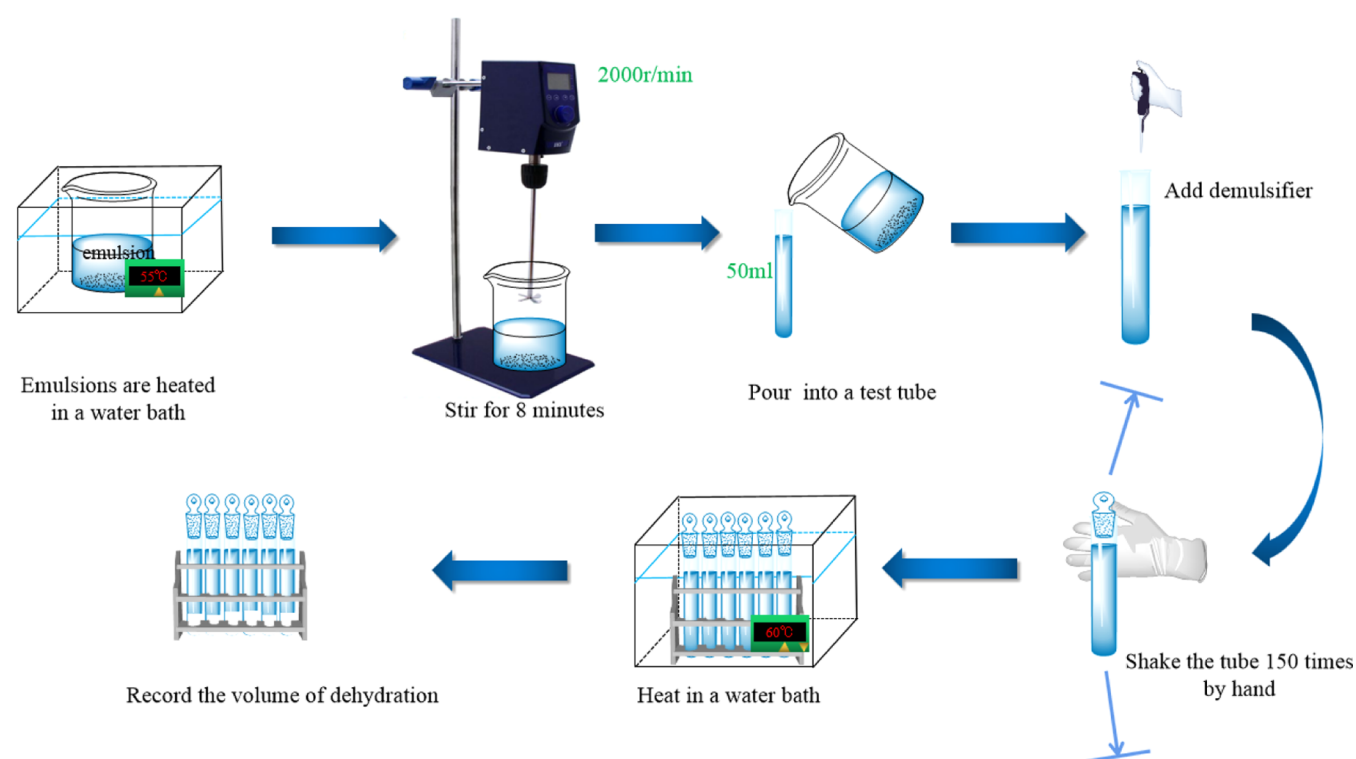


Figure 12. Schematic diagram of demulsification and water removal experiment.⁶⁵

The crude oil emulsion was placed in a constant-temperature water bath, heated to 55 °C for 30 min, and then put into a stirring motor for 8 min at a speed of 2000 r/min. After that, it was put into the stirring machine for 5 min. The crude oil emulsion (50 mL) was poured into a calibrated test tube, which was put into a water bath heated to 60 °C and kept at a constant temperature for 25 min. The height of the water surface should not exceed the height of the crude oil in the test tube. FB series polyether demulsifiers were added into the test tube with a micropipette and the cork was tightened. The test tube was turned upside down, shaken three to five times, and the cork was loosened to let off air. The bottle was recorked and the tube was shaken 150 times with hand to fully mix the demulsifier and crude oil emulsion. After the cork was capped, the bottle was placed in a water bath at 60 °C for settling. The volume of water removal at different time periods is observed, and the water removal (%) is calculated according to formula 3.⁶⁴

$$S = \frac{V_1 - V_0}{V \times W_v} \times 100\% \quad (3)$$

where S is the water removal (%) of demulsifier to heavy oil emulsion; V_0 is the amount of water discharged from blank control group; V is the emulsion volume of crude oil; and W_v is the emulsion volume moisture content of crude oil.

Figure 12 shows a schematic diagram of demulsification and water removal experiment.

Microscopic Demulsification Process Test. Heavy oil emulsion with 0.1 g/L FB 4 was evenly spread on glass slides at 25 °C. A BH-2 microscope was used for observation. Microdemulsifier processes at different time periods were performed using SPECTRUMSEE-ADVANCE software.

AUTHOR INFORMATION

Corresponding Author

Lin Zhang – School of Petroleum Engineering, Northeast Petroleum University, Daqing 163318, China; orcid.org/0000-0002-9740-1980; Email: 948689953@qq.com

Authors

Lixin Wei – School of Petroleum Engineering, Northeast Petroleum University, Daqing 163318, China; orcid.org/0000-0001-5596-8789

Shijun Guo – School of Petroleum Engineering, Northeast Petroleum University, Daqing 163318, China

Xinlei Jia – School of Petroleum Engineering, Northeast Petroleum University, Daqing 163318, China

Yu Zhang – School of Petroleum Engineering, Northeast Petroleum University, Daqing 163318, China

Chao Sun – Pipechina North Pipeline Company, Langfang 065000, China

Xuanrui Dai – School of Petroleum Engineering, Northeast Petroleum University, Daqing 163318, China; orcid.org/0000-0002-8775-8003

Complete contact information is available at: <https://pubs.acs.org/10.1021/acsomega.1c03530>

Notes

The authors declare no competing financial interest.

ACKNOWLEDGMENTS

The authors are grateful to the reviewers for their instructive suggestions and careful proofreading. This work was supported by the Natural Science Foundation of Shandong Province for Youth (grant no. ZR2020QE111), the Doctoral Research Startup Project of Binzhou University (grant no. 2019Y27),

and Postdoctoral Science Foundation of China (grant no. 2020M681073).

REFERENCES

- (1) Kamyk, J.; Kot-Niewiadomska, A.; Galos, K. The criticality of crude oil for energy security: a case of Poland. *Energy* **2021**, *220*, No. 119707.
- (2) Umar, M.; Su, C. W.; Rizvi, S.; Oana-Ramona, L. O. B. O. N. Driven by fundamentals or exploded by emotions: detecting bubbles in oil prices. *Energy* **2021**, *231*, No. 120873.
- (3) Sun, W.; Cheng, Q.; Zhao, L.; Li, Z.; Liu, Y. Energy loss analysis of the storage tank coil heating process in a dynamic thermal environment. *Appl. Therm. Eng.* **2021**, *189*, No. 116734.
- (4) Xu, X.; Cao, D.; Liu, J.; Gao, J.; Wang, X. Research on ultrasound-assisted demulsification/dehydration for crude oil. *Ultrason. Sonochem.* **2019**, *57*, 185–192.
- (5) Wang, Z. M.; Zhang, J. Corrosion of multiphase flow pipelines: the impact of crude oil. *Corros. Rev.* **2016**, *34*, 17–40.
- (6) Adewunmi, A. A.; Kamal, M. S. Demulsification of water-in-oil emulsions using ionic liquids: effects of counterion and water type. *J. Mol. Liq.* **2019**, *279*, 411–419.
- (7) Guzmán-Lucero, D.; Flores, P.; Rojo, T.; Martínez-Palou, R. Ionic liquids as demulsifiers of water-in-crude oil emulsions: study of the microwave effect. *Energy Fuels* **2010**, *24*, 3610–3615.
- (8) Velayati, A.; Nouri, A. Role of asphaltene in stability of water-in-oil model emulsions: the effects of oil composition and size of the aggregates and droplets. *Energy Fuels* **2021**, *35*, 5941–5954.
- (9) Elisângela, B. S.; Santos, D.; Alves, D. R. M.; Barbosa, M. S.; Guimarães, R. C. L.; Ferreira, B. M. S.; Guarnieri, R. A.; Franceschi, E.; Dariva, C.; Santos, A. F.; Fortuny, M. Demulsification of Heavy Crude Oil Emulsions Using Ionic Liquids. *Energy Fuels* **2013**, *27*, 6311–6315.
- (10) Wu, X. Investigating the stability mechanism of water-in-diluted bitumen emulsions through isolation and characterization of the stabilizing materials at the interface. *Energy Fuels* **2003**, *17*, 179–190.
- (11) Cloud, R. W.; Marsh, S. C.; Ramsey, B. L.; Pultz, R. A.; Poindexter, M. K. Salt spherulitic structures isolated from petroleum-based emulsions. *Energy Fuels* **2007**, *21*, 1350–1357.
- (12) Negi, H.; Faujdar, E.; Saleheen, R.; Singh, R. K. Viscosity modification of heavy crude oil by using a chitosan-based cationic surfactant. *Energy Fuels* **2020**, *34*, 4474–4483.
- (13) Adlakha, J.; Singh, P.; Ram, S. K.; Kumar, M.; Singh, M. P.; Singh, D.; et al. Optimization of conditions for deep desulfurization of heavy crude oil and hydrodesulfurized diesel by *Gordonia sp.* *Fuel* **2016**, *184*, 761–769.
- (14) Chen, Y.; He, H.; Yu, Q.; Liu, H.; Liu, W. Insights into enhanced oil recovery by polymer-viscosity reducing surfactant combination flooding in conventional heavy oil reservoir. *Geofluids* **2021**, *2021*, 1–12.
- (15) Ghanavati, M.; Shojaei, M. J.; Ahmad, R. Effects of asphaltene content and temperature on viscosity of Iranian heavy crude oil: experimental and modeling study. *Energy Fuels* **2013**, *27*, 7217–7232.
- (16) Wang, X.; Zhang, H.; Liang, X.; Shi, L.; Ye, Z.; et al. New amphiphilic macromolecule as viscosity reducer with both asphaltene dispersion and emulsifying capacity for offshore heavy oil. *Energy Fuels* **2021**, *35*, 1143–1151.
- (17) Zhao, Q.; Guo, L.; Wang, Y.; Jin, H.; Chen, L.; Huang, Z. Enhanced oil recovery and in situ upgrading of heavy oil by supercritical water injection. *Energy Fuels* **2020**, *34*, 360–367.
- (18) Raikos, V. Effect of heat treatment on milk protein functionality at emulsion interfaces. a review. *Food Hydrocolloids* **2010**, *24*, 259–265.
- (19) Souas, F.; Safri, A.; Benmounah, A. A review on the rheology of heavy crude oil for pipeline transportation. *Pet. Res.* **2021**, *6*, 116–136.
- (20) Piroozian, A.; Hemmati, M.; Ismail, I.; Manan, M. A.; Rashidi, M. M.; Mohsin, R. An experimental study of flow patterns pertinent to waxy crude oil-water two-phase flows. *Chem. Eng. Sci.* **2017**, *164*, 313–332.
- (21) Yi, M.; Huang, J.; Wang, L. Research on crude oil demulsification using the combined method of ultrasound and chemical demulsifier. *J. Chem.* **2017**, *2017*, 1–7.
- (22) Pradilla, D.; Ramirez, J.; Zanetti, F.; Alvarez, O. Demulsifier performance and dehydration mechanisms in Colombian heavy crude oil emulsions. *Energy Fuels* **2017**, *31*, 10369–10377.
- (23) Wang, Z.; Le, X.; Feng, Y.; Hu, Z. Dehydration of aging oil by an electrochemical method. *Chem. Technol. Fuels Oils* **2014**, *50*, 262–268.
- (24) Hjartnes, T. N.; Sreland, G. H.; Simon, S. C.; Sjoblom, J. Demulsification of crude oil emulsions tracked by pulsed field gradient nmr. part i: chemical demulsification. *Ind. Eng. Chem. Res.* **2019**, *58*, 2310–2323.
- (25) Wang, D.; Yang, D.; Huang, C.; Huang, Y.; Zeng, H.; et al. Stabilization mechanism and chemical demulsification of water-in-oil and oil-in-water emulsions in petroleum industry: a review. *Fuel* **2021**, *286*, No. 119390.
- (26) Shehzad, F.; Hussein, I. A.; Kamal, M. S.; Ahmad, W.; Nasser, M. S.; Sultan, A. S. Polymeric surfactants and emerging alternatives used in the demulsification of produced water: a review. *Polym. Rev.* **2018**, *58*, 63–101.
- (27) Sun, H.; Wang, Q.; Li, X.; He, X. Novel polyether-polyquaternium copolymer as an effective reverse demulsifier for o/w emulsions: demulsification performance and mechanism. *Fuel* **2020**, *263*, 116770.
- (28) Wu, M.; Zhai, M.; Li, X. Adsorptive removal of oil drops from asp flooding-produced water by polyether polysiloxane-grafted zif-8. *Powder Technol.* **2021**, *378*, 76–84.
- (29) Li, X.; Ma, J.; Bian, R.; et al. Novel polyether for efficient demulsification of interfacially active asphaltene-stabilized water-in-oil emulsions. *Energy Fuels* **2020**, *34*, 3591–3600.
- (30) Al-Sabagh, A. M.; El-Din, M. N.; Fotouh, A. E.; Nasser, N. M. Investigation of the demulsification efficiency of some ethoxylated polyalkylphenol formaldehydes based on locally obtained materials to resolve water-in-oil emulsions. *J. Dispersion Sci. Technol.* **2009**, *30*, 267–276.
- (31) Wang, J.; Hu, F.-L.; Li, C.-Q.; Li, J.; Yang, Y. Synthesis of dendritic polyether surfactants for demulsification. *Sep. Purif. Technol.* **2010**, *73*, 349–354.
- (32) Chakrabarti, C.; Khimani, M.; Patel, V.; Parekh, P.; Muddassir, M.; et al. Solubilization of polycyclic aromatic hydrocarbons (pahs) in peo-ppo-peo type linear and star block copolymers. *J. Mol. Liq.* **2021**, *325*, 115177.
- (33) Hsiao, F.; Huang, P.-Y.; Aoyagi, T.; Chang, S.-F.; Liaw, J. In vitro and in vivo assessment of delivery of hydrophobic molecules and plasmid DNAs with peo-ppo-peo polymeric micelles on cornea. *J. Food Drug Anal.* **2018**, *26*, 869–878.
- (34) Yang, S.; Zhang, Z.; Wang, F.; Feng, L.; Jiang, X.; Yang, C.; et al. The synthesis and the bulk rheological properties of the highly-branched block polyethers. *Polym. Sci., Ser. A* **2014**, *56*, 917–927.
- (35) Jung, H.-S.; Park, Y.; Nah, C.-W.; Lee, J.-C.; Kim, K.-Y.; Lee, C. S. Evaluation of the mechanical properties of polyether sulfone-toughened epoxy resin for carbon fiber composites. *Fibers Polym.* **2021**, *22*, 184–195.
- (36) Hirao, A.; Hayashi, M.; Loykulnant, S.; Sugiyama, K.; Sang, W. R.; Haraguchi, N.; et al. Precise syntheses of chain-multi-functionalized polymers, star-branched polymers, star-linear block polymers, densely branched polymers, and dendritic branched polymers based on iterative approach using functionalized 1,1-diphenylethylene derivatives. *Prog. Polym. Sci.* **2005**, *30*, 111–182.
- (37) Alves, A. V.; Tsiannou, M.; Alexandridis, P. Fluorinated surfactant adsorption on mineral surfaces: implications for PFAS fate and transport in the environment. *Surfaces* **2020**, *3*, 516–566.
- (38) Zhang, D. Q.; Zhang, W. L.; Liang, Y. N. Adsorption of perfluoroalkyl and polyfluoroalkyl substances (PFAS) from aqueous solution—a review. *Sci. Total Environ.* **2019**, *694*, 133606.
- (39) Frömel, T.; Knepper, T. P. Biodegradation of fluorinated alkyl substances. In *Reviews of Environmental Contamination and Toxicology*; Springer, 2010; Vol. 208, pp 161–177.

- (40) Reiner, J. L.; Blaine, A. C.; Higgins, C. P.; Huset, C.; Keller, J. M.; et al. Polyfluorinated substances in abiotic standard reference materials. *Anal. Bioanal. Chem.* **2015**, *407*, 2975.
- (41) Drouiche, N.; Ghaffour, N.; Lounici, H.; Mameri, N.; Maallemi, A.; Mahmoudi, H. Electrochemical treatment of chemical mechanical polishing wastewater: removal of fluoride-sludge characteristics - operating cost. *Desalination* **2008**, *223*, 134–142.
- (42) Sha, Q.; Xie, H.; Liu, W.; Yang, D.; Ge, C.; et al. Removal of fluoride using platanus acerifoli leaves biochar an efficient and low-cost application in wastewater treatment. *Environ. Technol.* **2021**, 1–15.
- (43) Bélarbi, H.; Bendedouch, D.; Bouanani, F. Mixed micellization properties of nonionic fluorocarbon/cationic hydrocarbon surfactants. *J. Surfactants Deterg.* **2010**, *13*, 433–439.
- (44) Zhang, J.; Wang, Y.; Xu, G.; Lin, M.; Fan, T.; Yang, Z.; Dong, Z. Formation and rheological behavior of wormlike micelles in a catanionic system of fluoroacetic acid and tetradecyldimethylaminoxide. *Soft Matter* **2017**, *13*, 670–676.
- (45) Peyre, V. Segregation phenomena in micelles from mixtures of fluorinated and hydrogenated surfactants. *Curr. Opin. Colloid Interface Sci.* **2009**, *14*, 305–314.
- (46) Song, N.; Huang, X.; Li, Y.; Zhang, K.; Wei, C.; Zhang, J.; Zhang, Y. Synthesis and application of new multibranched-linear-multibranched fluorinated copolymer as demulsifiers for naphthenic compounds stabilized emulsion. *J. Fluorine Chem.* **2021**, *249*, No. 109842.
- (47) Xu, H.; Jia, W.; Ren, S.; Wang, J.; Yang, S. Stable and efficient demulsifier of functional fluorinated graphene for oil separation from emulsified oily wastewaters. *J. Taiwan Inst. Chem. Eng.* **2018**, *93*, 492–499.
- (48) Zhang, D.; Sha, M.; Pan, R.; et al. Synthesis and properties study of novel fluorinated surfactants with perfluorinated branched ether chain. *J. Fluorine Chem.* **2019**, *219*, 62–69.
- (49) Du, Y.; Zhou, Z. H.; Gao, M.; Han, L.; Zhang, L.; Yan, F.; et al. Adsorption and wettability of extended anionic surfactants with different po numbers on a polymethylmethacrylate surface. *Soft Matter* **2021**, *17*, 6426–6434.
- (50) Lv, W.; Gong, H.; Li, Y.; Qian, S.; Xu, L.; Dong, M. Dissolution behaviors of alkyl block polyethers in co₂: experimental measurements and molecular dynamics simulations. *Chem. Eng. Sci.* **2020**, *228*, No. 115953.
- (51) Pereira, J. C.; Delgado-Linares, J.; Scorzza, C.; Rondo, N. M.; Rodri Guez, S.; Salager, J. L. Breaking of water-in-crude oil emulsions. 4. estimation of the demulsifier surfactant performance to destabilize the asphaltenes effect. *Energy Fuels* **2011**, *25*, 1045–1050.
- (52) Zaltarov, M.-F.; Filip, D.; Macocinschi, D.; et al. Self-assembly and rheological behavior of chloramphenicol-based poly(ester ether)-urethanes. *J. Polym. Res.* **2021**, *28*, No. 190.
- (53) Shi, Y.; Luo, H. Q.; Li, N. B. Determination of the critical premicelle concentration, first critical micelle concentration and second critical micelle concentration of surfactants by resonance rayleigh scattering method without any probe. *Spectrochim. Acta, Part A* **2011**, *78*, 1403–1407.
- (54) Lv, K.; Jia, K.; Yang, Y.; Huang, W.; Wu, H.; Pan, W.; Jia, H. Effects of additional salts on the interfacial tension of crude oil/zwitterionic gemini surfactant solutions. *J. Dispersion Sci. Technol.* **2019**, *40*, 1031–1038.
- (55) Pang, J.; Zhao, T.; Xin, X.; Chen, Y.; Tan, Y.; Xu, G. Effect of inorganic salts on the aggregation behavior of aot at the air/water interface. *J. Surfactants Deterg.* **2016**, *19*, 1015–1024.
- (56) Pericet-Camara, R.; Papastavrou, G.; Behrens, S. H.; Helm, C. A.; Borkovec, M. Interaction forces and molecular adhesion between pre-adsorbed poly(ethylene imine) layers. *J. Colloid Interface Sci.* **2006**, *296*, 496–506.
- (57) Liu, J.; Zhong, L.; Yuan, X.; Liu, Y.; Zhang, H.; et al. Study on the re-emulsification process of water in heavy oil emulsion with addition of water-soluble viscosity reducer solution. *Energy Fuels* **2019**, *33*, 10852–10860.
- (58) Sakuma, H.; Kondo, T.; Nakao, H.; Shiraki, K.; Kawamura, K. Structure of hydrated sodium ions and water molecules adsorbed on the mica/water interface. *J. Phys. Chem. C* **2011**, *115*, 15959–15964.
- (59) Raikos, V. Effect of heat treatment on milk protein functionality at emulsion interfaces. a review. *Food Hydrocolloids* **2010**, *24*, 259–265.
- (60) Feng, X.; Mussone, P.; Gao, S.; Wang, S.; Wu, S. Y.; Masliyah, J. H.; Xu, Z. Mechanistic study on demulsification of water-in-diluted bitumen emulsions by ethylcellulose. *Langmuir* **2010**, *26*, 3050–3057.
- (61) Pensini, E.; Harbottle, D.; Yang, F.; Tchoukov, P.; Li, Z.; Kailey, I.; Behles, J.; Masliyah, J.; Xu, Z. Demulsification mechanism of asphaltene-stabilized water-in-oil emulsions by a polymeric ethylene oxide-propylene oxide demulsifier. *Energy Fuels* **2014**, *28*, 6760–6771.
- (62) Wang, J.; Li, C. Q.; An, N.; Yang, Y. Synthesis and demulsification of two lower generation hyperbranched polyether surfactants. *Sep. Sci. Technol.* **2012**, *47*, 1583–1589.
- (63) Gotsche, M.; Wood, C.; Tiefensee, K. Preparation of W/O emulsions. US Patent US6,444,785B1, 2002.
- (64) Kailey, I. Key performance indicators reveal the impact of demulsifier characteristics on oil sands froth treatment. *Energy Fuels* **2017**, *31*, 2636–2642.
- (65) Wei, L.; Zhang, L.; Chao, M.; Jia, X.; Liu, C.; Shi, L. Synthesis and study of a new type of nonanionic demulsifier for chemical flooding emulsion demulsification. *ACS Omega* **2021**, *6*, 17709–17719.